

High Current Lanthanum Hexaboride Hollow Cathodes for High Power Hall Thrusters

IEPC-2011-053

*Presented at the 32nd International Electric Propulsion Conference,
Wiesbaden • Germany
September 11 – 15, 2011*

Dan M. Goebel¹ and Emily Chu²
Jet Propulsion Laboratory, California Institute of Technology, Pasadena CA 91109 USA Third Author³

Abstract: Space missions continue to demand higher power Hall and ion thrusters capable of providing high thrust and long life. For high power Hall thrusters in the range of 20 to 100-kW being developed for future cargo and manned-missions, the hollow cathodes will be required to produce discharge currents of 50 to 400 A with lifetimes in excess of 10 khrs. A lanthanum hexaboride (LaB6) hollow cathode has been previously developed for space applications that features graphite tubes or sleeves to provide a diffusion boundary to protect the LaB6 insert from chemical reactions with the refractory metals, and includes a long life heater capable of igniting the higher temperature emitter. Several versions of this cathode design with different LaB6 insert diameters have been built and tested at up to 250 A of discharge current to demonstrate both the high current capability and ease of handling and gas purity requirements obtained with LaB6 cathodes. While the LaB6 cathode insert operates at a higher temperature than the conventional BaO dispenser cathode, LaB6 offers the capability of very high discharge currents, long life and orders of magnitude less sensitivity to propellant impurities and air exposure than conventional dispenser cathodes.

Nomenclature

A	=	theoretical coefficient in the Richardson-Dushman thermionic emission equation
d	=	cathode inside diameter
D	=	diffusion coefficient
D _a	=	ambipolar diffusion coefficient
D _o	=	experimentally modified value of A
e	=	electron charge
f _n	=	edge to average plasma density ratio in insert region
H	=	cathode heat loss
I _c	=	hollow cathode discharge current
I _i	=	ion current in the insert region
I _r	=	random electron flux
k	=	Boltzman's constant
l	=	disk length in gas flow model
m	=	electron mass
M	=	ion mass
n _o	=	neutral density
T	=	temperature

¹ Senior Research Scientist, Advanced Propulsion Group, Jet Propulsion Laboratory, dan.m.goebel@jpl.nasa.gov

² Graduate Student, University of California Los Angeles, Jet Propulsion Laboratory Internship, emily.chu@jpl.nasa.gov

T_e	=	electron temperature
T_i	=	ion temperature
T_r	=	temperature normalized to 289.7 K
$P_{1,2}$	=	pressure
Q	=	xenon gas flow rate
r	=	insert radius
R	=	plasma resistance
U^+	=	ionization potential
V	=	plasma volume
v_{scat}	=	effective velocity for ion scattering
α	=	temperature coefficient of the material work function
ζ	=	gas viscosity
λ_{01}	=	first zero of the Bessel function
σ_i	=	ionization cross section
σ_{CEX}	=	charge exchange cross section
ϕ_{wf}	=	work function
ϕ_o	=	temperature independent work function
ϕ_s	=	sheath voltage in the cathode insert region

I. Introduction

There is a growing interest in NASA in using electric propulsion to reduce launch vehicle size and facilitate in-space transportation of large masses in support of the newly emerging vision for the manned space program^{1,2}. The success of electric propulsion thrusters in prime propulsion and ACS applications in several recent missions^{3,4,5} has also prompted additional concepts⁶ to emerge for electric propulsion missions using higher power ion and Hall thrusters capable of providing high thrust and long life. The next generation Hall thrusters being developed for these high power applications in the range of 20 to 100-kW will require hollow cathodes to produce discharge currents of 50 to 400 A with lifetimes in excess of 10 khrs. NASA and the commercial aerospace industry in the US have spent many years developing and ultimately flying barium-oxide impregnated dispenser cathodes in various ion thrusters, Hall thrusters, plasma contactors, and plasma neutralizers at discharge currents under 25 A. These cathodes use a porous tungsten insert that is impregnated with an emissive mix of barium and calcium oxides and alumina^{3,4}. This configuration is called a dispenser cathode because the tungsten matrix acts as a reservoir for barium that is “dispensed” from the pores to activate the emitter surface. Chemical reactions in the pores or at the surface at high temperature evolve a barium oxide dipole attached to an active site on the tungsten substrate, which reduces the work function of the surface to about 2.06 eV at temperatures in excess of 1000 °C. Because chemistry is involved in the formation of the low work function surface, dispenser cathodes are subject to poisoning that can significantly increase the work function⁸. Care must be taken in handling the inserts and in the vacuum conditions used during operation and storage of these cathodes to avoid poisoning by water vapor and impurities in the gas that can shorten the lifetime or even prevent cathode emission. One of the major drawbacks of using BaO dispenser cathodes in electric propulsion applications is the extremely high feed gas purity presently specified by NASA and commercial ion thruster manufacturers to avoid these poisoning issues, which has resulted in a special “propulsion-grade” xenon with overall >99.999% purity and ≤ 0.1 -ppm oxygen and water impurity specifications⁹, and extensive spacecraft feed system cleaning techniques to be required. Finally, increasing the discharge current capability of BaO-W dispenser hollow cathodes to over 50-to-100 A typically results in overheating of the insert and reduced life.

An alternative electron emission material with a vast amount of use in both space and on the ground is lanthanum hexaboride (LaB₆). Over a hundred Russian Hall thrusters have been flown over the last 35 years with LaB₆ cathodes^{10,11}, and Russian SPT-100 thrusters with LaB₆ hollow cathodes have recently been used on several Loral communication satellites for station keeping^{12,13}. LaB₆ electron emitters are also used extensively in university research devices and many industrial applications such as plasma sources, ion sources, arc melters, optical coaters, ion-platers, scanning electron microscopes, and many other applications. Recently, several high-current LaB₆ hollow cathodes have been developed at JPL for high power Hall thrusters¹⁴⁻¹⁶.

The major reason for using LaB₆ cathodes, as compared to conventional impregnated dispenser cathodes, is the incredible robustness, high current density and long life exhibited by LaB₆ electron emitters. Lanthanum hexaboride cathodes are routinely used in all noble gases from helium to xenon, reactive gases including hydrogen and oxygen, and various other materials including liquid metals such as bismuth. LaB₆ cathodes have even been successfully used in oxygen and nitrogen plasma discharges at emission current densities exceeding 20 A/cm², and vented to

water vapor (from cooling lines breaking) and air during operation without damaging the cathode. The space heritage of LaB₆ cathodes in Russian and US spacecraft is considerable, and the industrial experience in dealing with the higher operating temperatures and materials compatibility issues is extensive.

Lanthanum hexaboride¹⁷ is a crystalline material made by press-sintering LaB₆ powder into rods or plates and then electron-discharge machining the material to the desired shape. Polycrystalline LaB₆ cathodes have a work function of about 2.67 eV depending on the surface stoichiometry¹⁸, and will emit over 10 A/cm² at a temperature of 1650 °C. Since the bulk material is emitting, there is no chemistry involved in establishing the low work function surface and LaB₆ cathodes are insensitive to impurities and air exposures that would normally destroy a BaO dispenser cathode. In addition, the cathode life is determined primarily by the evaporation rate of the bulk LaB₆ material at typical operating temperatures¹⁹⁻²¹. The higher operating temperature of LaB₆ and the need to make contact with LaB₆ with compatible materials has perhaps unjustly limited their use in the US space program.

To provide the high discharge current and long life desired for the next generation high power Hall thrusters, the LaB₆ hollow cathodes previously developed at JPL have been modified and tested to higher current levels. In addition, internal plasma measurements were made at discharge currents up to 100 A to aid in designing and modeling for higher power. Three different sizes of the basic cathode design have been built to provide various current ranges and to fit into different thruster sizes. The designs all utilize a LaB₆ insert in a hollow tube made of either graphite or a refractory metal such molybdenum, with a tungsten orifice plate and an Al₂O₃ insulated, tantalum sheathed heater. The cathodes use graphite sleeves to interface the LaB₆ with the supporting structure, and also have a graphite keeper. The smaller version of this cathode has been operated in xenon from 5 A to 60 A continuously, and the larger versions tested at discharge currents of up to 250 A. In this paper, the characteristics of LaB₆ and the hollow cathode configurations that use this material are described. In addition, life estimates for the cathodes and information on issues associated with testing at high current are presented and discussed.

II. LaB₆ Characteristics

Lanthanum hexaboride was first developed as an electron emitter by Lafferty¹⁷ in the 1950's. The thermionic emission of lanthanum-boron compounds as a function of the surface stoichiometry was studied by several authors¹⁸⁻²¹. The Russian SPT Hall thrusters¹¹, flown since 1971, all utilize LaB₆ cathodes. Lanthanum hexaboride was first used in the US in a hollow cathode in 1978²², and the development of a high-current LaB₆ cathode for plasma sources that dealt with supporting and making electrical contact with the material was described²³ in 1985. The lanthanum-boron system can consist of combinations of stable LaB₄, LaB₆, and LaB₉ compounds, with the surface color determined by the dominate compound²⁰. The evolution of LaB₄ to LaB₉ compounds is caused either by preferential sputtering of the boron or lanthanum atoms at the near surface by energetic ion bombardment²⁰, or by preferential chemical reactions with the surface atoms^{18,19}. Lanthanum-boride compounds, heated to in excess of 1000 °C in vacuum, evaporate their components at a rate that produces a stable LaB_{6,0} surface.

Thermionic emission by these cathode materials is described well by the Richardson-Dushman equation²⁴:

$$J = AT^2 e^{\frac{-e\phi_{wf}}{kT}} \quad (1)$$

where A is a constant with a value of 120 A/cm²K² and ϕ_{wf} is the work function. Experimental investigations of the thermionic emission of different materials report values of A that vary considerably from the theoretical value. This has been handled by a temperature correction for the work function of the form²⁵

$$\phi_{wf} = \phi_o + \alpha T, \quad (2)$$

where ϕ_o is the classically reported work function at absolute zero and α is an experimentally measured constant. This dependence can be inserted into Eq. 1 to give

$$J = Ae^{\frac{-e\alpha}{k}} T^2 e^{\frac{-e\phi_o}{kT}} = D_o T^2 e^{\frac{-e\phi_o}{kT}}, \quad (3)$$

where D_o is the temperature-modified coefficient to the Richardson-Dushman equation.

Several different work functions have been reported in the literature for LaB₆. This is primarily due to varying use of A or D_o in Eq. 3, variations in the surface stoichiometry¹⁸, or due to different densities of polycrystalline LaB₆

emitters or crystal orientations in single-crystal emitters used for some applications²¹. For hollow cathode and large area emitter applications, LaB₆ emitters are usually fabricated by press-sintering powder to produce polycrystalline material with a work function that is an average over the different crystal orientations at the surface. Table 1 shows the work function and values of A and D₀ for different electron emitter materials given in the literature. The emission current density calculated from Eq. 3 for the materials in Table 1 are plotted in Figure 1 as a function of emitter temperature. Amazingly, the actual emission current density of LaB₆ predicted by the different authors in Table 1 is within about 25% for the different values of A, D₀ and φ_{wf} used. LaB₆ operates at several hundred degrees higher temperature than BaO-W dispenser cathodes for the same emission current density. The LaB₆ temperature is also much lower than the typical refractory metal emitters used for filaments in some plasma discharges.

Lanthanum hexaboride offers long lifetimes because its evaporation rate is significantly lower than refractory metals at thermionic emission temperatures. Figure 2 shows the evaporation rate of LaB₆ and tungsten as a function of the emission current density^{26,27}. LaB₆ evaporation is more than one order of magnitude lower when compared to tungsten at the same emission current density. For comparison, the evaporation rate of BaO from a Type-S 411 dispenser cathode⁸ is also shown. In spite of operating at a significantly higher temperature, the LaB₆ has a lower evaporation rate than the impregnate material in dispenser cathodes until the emission current exceeds about 15 A/cm². This illustrates why the LaB₆ cathode life is usually better than BaO-W cathodes because there is more material in the bulk LaB₆ than in the impregnated dispenser cathodes, and the evaporation rate is lower or comparable up to about 20 A/cm².

Lafferty pointed out in his original 1951 paper¹⁷ that LaB₆ must be supported by materials that inhibit diffusion of boron into the support material, which embrittles most of the contacting refractory metals that can be used at the higher operating temperatures of LaB₆ and lead to structural failure. In addition, the crystalline LaB₆ is susceptible to breakage from mechanical stress when clamped and from thermal shock. LaB₆ has been supported by carbon^{22,23}, tantalum carbide^{17,27}, and rhenium²⁸ to avoid these problems, or constructed support structures with the interface material at lower temperatures²⁹. Fine-grain graphite has a comparable coefficient of thermal expansion¹⁵ as LaB₆, and provides good electrical contact and low stress support^{16,23} without significant boron diffusion or boride formation. For this reason, the hollow cathodes described here use Poco graphite in contact with a LaB₆ insert.

Comprehensive investigations into the poisoning of dispenser cathodes³⁰ and LaB₆ cathodes³¹ have been published in the literature. The most potent poisons for both cathodes are oxygen and water, with other gases such as

Table 1. Work function and Richardson coefficients for different cathode materials.

	A	D ₀	φ _{wf}
BaO-W 411 [8]	120		1.67 + 2.82x10 ⁻⁴ T
BaO-W 411 [14]		1.5	1.56
LaB ₆ [17]		29	2.67
LaB ₆ [20]		110	2.87
LaB ₆ [18]	120		2.91
LaB ₆ [26]	120		2.66 + 1.23x10 ⁻⁴ T
Molybdenum [26]		55	4.2
Tantalum [26]		37	4.1
Tungsten [26]		70	4.55

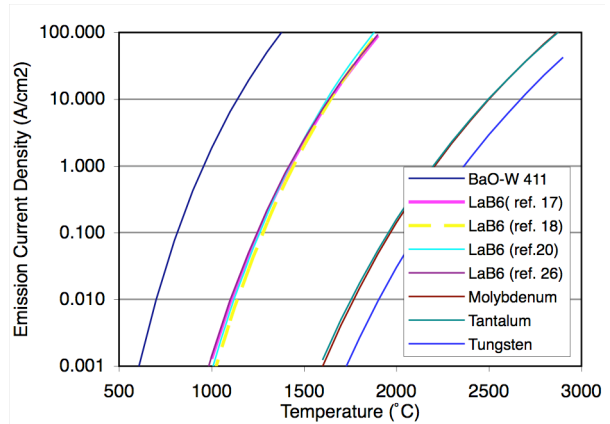


Figure 1. Emission current density versus temperature.

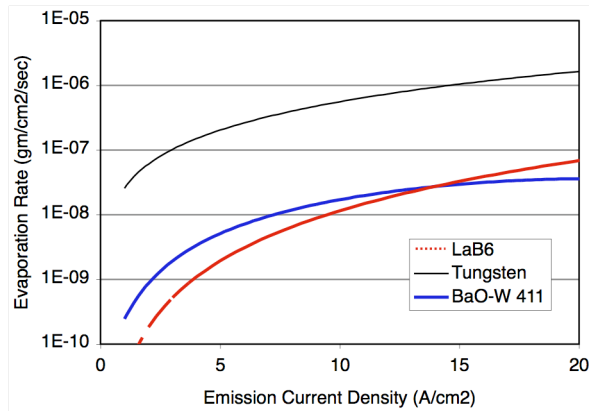


Figure 2. Evaporation rate of LaB₆ compared to tungsten and Type-B dispenser cathodes.

CO₂ and air causing poisoning at higher partial pressures. Figure 3 shows the fraction of the possible thermionic emission given by Eq. 3 for a dispenser cathode and LaB₆ is plotted as a function of the partial pressures of oxygen and water for several different emitter temperatures. LaB₆ is significantly less sensitive to impurities that tend to limit the performance and life of the barium dispenser cathodes. The curve for water poisoning²⁰ of LaB₆ is off the graph to the right at much higher partial pressures. We see that a partial pressure of oxygen below 10⁻⁶ Torr in the background or feed gas exposed to a dispenser cathode at temperatures of up to 1100 °C will cause significant degradation in the vacuum electron emission. In a similar manner, water vapor at partial pressures below 10⁻⁵ Torr will poison dispenser cathodes at temperatures below 1110 °C. For typical pressures inside hollow cathodes of in excess of 1 Torr, this partial pressure then represents the best purity level that can be achieved by the gas suppliers, resulting in the high “propulsion-grade” purity mentioned above.

In contrast, LaB₆ at 1570 °C, where the electron emission current density is nearly the same as for the dispenser cathode at 1100 °C, can withstand oxygen partial pressures up to 10⁻⁴ Torr without degradation in the electron emission. This means that LaB₆ can tolerate two orders of magnitude higher impurity levels in the feed gas compared to dispenser cathodes. For the case of xenon ion thrusters, LaB₆ cathodes can tolerate the crudest grade of xenon commercially available (~99.99% purity) without affecting the LaB₆ electron emission or life. Lanthanum hexaboride cathodes also do not require any significant conditioning, activation or purging procedures that are normally required by dispenser cathodes. This robustness makes the handling and processing of thrusters that use LaB₆ cathodes significantly easier than electric propulsion devices that use dispenser cathodes.

III. Experimental Configuration

The LaB₆ hollow cathodes described here for space applications are configured in a geometry similar to conventional space dispenser hollow cathodes, which basically consists of an active thermionic insert placed inside a structural cathode tube wrapped by a heater, heat shields and keeper electrode. However, LaB₆ cathodes typically need more heater power to achieve the higher emission temperatures. BaO dispenser cathodes commonly use a coiled tantalum sheathed heater^{32,33} that utilizes a magnesium-oxide powder insulation. This insulation material has a maximum operation temperature typically less than 1400 °C, at which chemical reactions between the oxide insulation and the heater electrode or sheath material cause a reduction in the resistance and ultimately failure of the heater³³. A tantalum sheathed-heater that incorporates high-temperature alumina power insulation was procured³⁴ and used to heat the LaB₆ cathode. This geometry can be found in the standard catalog of several companies. The heater catalogs indicate that the alumina insulation has a maximum temperature of about 1800 °C, which is well in excess of the temperature required to start the LaB₆ cathode. The swaged tantalum heaters reliably provide about 200 W of heater power for the 1.5-cm-dia. cathode and 340 W of heater power used to light the 2-cm-dia. cathode. The 2.4-mm-dia. Ta-sheathed heaters have excellent life if the heater current is constrained to 11 A or less.

As mentioned above, the material in contact with the LaB₆ insert is typically made of graphite because it has a similar coefficient of thermal expansion^{26,35} as LaB₆. The cathode tube can either be made from Poco graphite, or from a refractory metal such as molybdenum with graphite sleeves used to interface with and contact the LaB₆ insert. A schematic representation of this generic configuration for the hollow cathode is shown in Fig. 4. The keeper

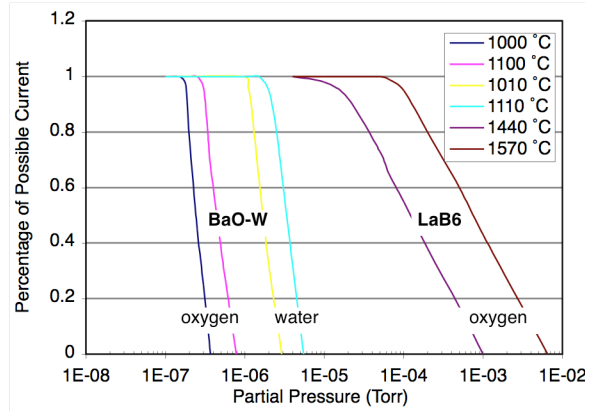


Figure 3. Percentage of possible thermionic emission versus partial pressure of oxygen and water showing the poisoning of dispenser cathodes relative to LaB₆ cathodes.

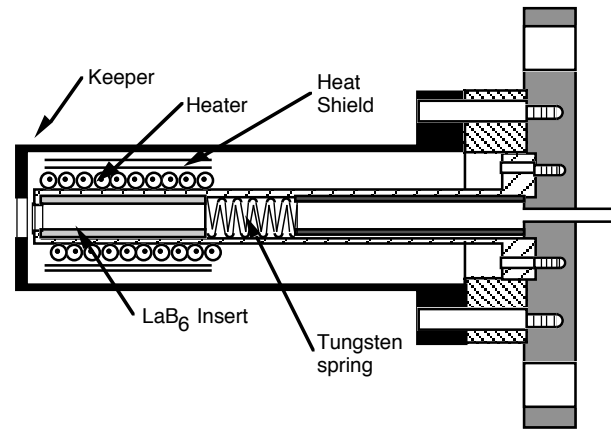


Figure 4. LaB₆ hollow cathode schematic.

electrode used to start the discharge is also fabricated from Poco graphite. The LaB₆ emitter is configured as an insert and is placed inside the hollow tube. The tube is sufficiently long and thin to minimize conduction of heat from the insert to the base plate. Cathodes of this design have been fabricated from 6 cm to 15 cm long for applications in different thrusters that require various cathode lengths. A cathode of this type was previously described in detail¹⁶ and operated at discharge currents of 5 to 60 A. The insert in this case has an outer diameter of 0.64 cm, an inside diameter of 0.38 cm, and a length of 2.5 cm. This provides 3 cm² of emission area exposed to the plasma in the hollow cathode, which at an insert temperature of 1700 °C can emit 20 A/cm² and a total current of about 60 A. The cathode orifice diameter was 80% of the insert inside diameter, and the Poco-graphite keeper orifice diameter was 0.64 cm. The insert is held in place with a tungsten spring placed inside the tube. A photograph of the cathode as configured to use in a Hall thruster is shown in Fig. 5.

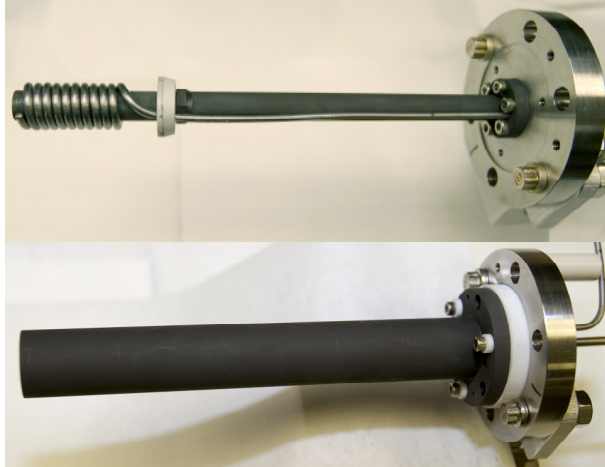


Figure 5. LaB₆ hollow cathode designed for Hall thrusters. Top photo shows the cathode tube and heater assembly, and the bottom photo shows the cathode assembly with the keeper installed.

The topic of this paper is the performance of two larger diameter LaB₆ hollow cathodes at higher discharge currents. The construction of these larger cathodes using the basic design illustrated in Fig. 4 has been previously described^{14,15}. The first cathode has a 1.5-cm O.D. graphite tube 7.6-cm long that holds a 1.27cm-dia. LaB₆ insert. The cathode tube has a wall thickness of about 0.1 cm, and the LaB₆ insert has a wall thickness of 0.32 cm and a length of 2.5 cm. This insert then has an active emitting area inside the cathode of about 5 cm², which according to Fig. 1 can produce emission currents of 100 A at temperatures of about 1700 °C. The graphite cathode tube eliminates interface issues with the LaB₆, and a tungsten orifice plate is inserted in the tube and held in place against a step at the tube end by the spring tension of tungsten spring. A thin graphoil washer is used to isolate the tungsten orifice plate from the LaB₆ insert. The graphite cathode tube and the keeper are bolted through insulating flanges that are attached to the gas feed system and the power supply electrical leads. Experiments with the cathode heater and different tube lengths showed that the heater power required to start the discharge could be reduced from 300 W for the 7.6-cm long tube to 240 W for a 10.7-cm tube length due to the reduction in the heat conducted to the mounting flange. Figure 6 shows a photograph of the 10.7-cm long, 1.5-cm dia. tube, LaB₆ cathode mounted on the test fixture with the alumina-insulated Ta-sheathed-heater and heat shielding wrapped around the cathode tube. As will be discussed below, this cathode was fully tested at its nominal discharge currents of 100 A, and then tested at discharge currents up to 200 A to determine the cathode failure mechanisms.



Figure 6. The 1.5-cm dia. LaB₆ hollow cathode with heater and heat shield installed, but without the keeper installed.

An additional larger cathode was also fabricated from this basic design. The larger diameter cathode features more insert surface area that required to provide higher discharge currents and long life. This cathode features a 2-cm-dia. by 10.7-cm-long graphite cathode tube with the same tube wall and insert thicknesses as the 1.5-cm cathode. The graphite tube holds a 1.9cm-dia. LaB₆ insert with a nominal length is 2.5 cm, but an additional insert can be installed to increase the length of the emitting region up to 5 cm long. The graphite keeper for this cathode has an outer

diameter of 3.5 cm to accommodate the larger cathode and the heater and heat shields. This cathode uses two of the Al_2O_3 insulated sheathed heaters connected in parallel around the cathode tube to provide the 300 W of heater power needed to light it. The mounting and spring geometry are the similar to the 1.5-cm cathode. A photograph of the larger cathode is shown in Fig. 7.

The cathodes were operated in the JPL cathode test facility³⁶ at discharge currents up to 100 A, which was limited by the power supply. This provided an initial characterization of the performance, and also permitted internal plasma density, potential and electron temperature profiles to be obtained for the 1.5-cm-dia. cathode. Both cathodes were then operated in a second facility that was configured as shown in Fig. 8 for discharge currents of up to 250 A. The facility has a 1-m-dia. by 2.5-m-long vacuum system with 1250 l/sec xenon pumping speed from two cryo-pumps. A solenoid coil is positioned around the keeper electrode to provide an adjustable axial magnetic field at the cathode exit. The anode consists of a water-cooled cone of relatively large area. This test configuration produces discharge voltages in the 15 to 40 V range, depending on the current and gas flow rate. Temperature measurements of the cathode orifice plate are made using a DFP 2000 Disappearing Filament Optical Pyrometer calibrated by a tungsten filament reference in the vacuum system. A comparison of the measured temperature of the filament to that derived from simple radiation theory was used to obtain a calibration curve to correct pyrometer temperature readings of the orifice plate through the vacuum system window.

IV. LaB_6 Cathode Discharge Performance

After installation in either of the test facilities, the systems were pumped down into the 10^{-6} Torr range and the cathode heater turned on for 10 minutes. The cathode discharge was then started by initiating the xenon gas flow through the cathode, applying 150 V to the keeper electrode and turning on the anode power supply. The keeper current was regulated to 2 A, and the keeper voltage fell to a value typically in the 5 to 10 V range depending on the gas flow rate and keeper orifice diameter. Once the anode discharge current exceeded 10 A, the keeper power supply was turned off and the keeper was allowed to float. The cathodes were normally run at 20 A for a minute or two until the discharge voltage stabilized, and then could be turned up to full current in a matter of seconds.

A. 1.5-cm Cathode Performance

Figure 9 shows the discharge voltage (a) and keeper voltage (b) versus discharge current for the 1.5-cm cathode measured for currents of 10 to 100 A and three xenon gas flow rates. At discharge currents below 20 A, the discharge voltage was observed to increase and both large cathodes tended to cool off and stop operating at currents below 10 A. This is because the self-heating mechanism in the hollow cathode depends on the discharge current level, and the lower discharge currents provided insufficient heating in these cathodes to maintain the insert



Figure 7. The 2-cm OD tube LaB_6 hollow cathode with the keeper mounted.

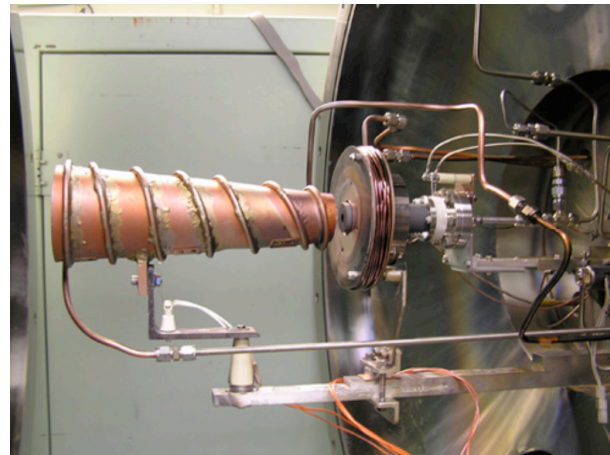


Figure 8. High current cathode test facility.

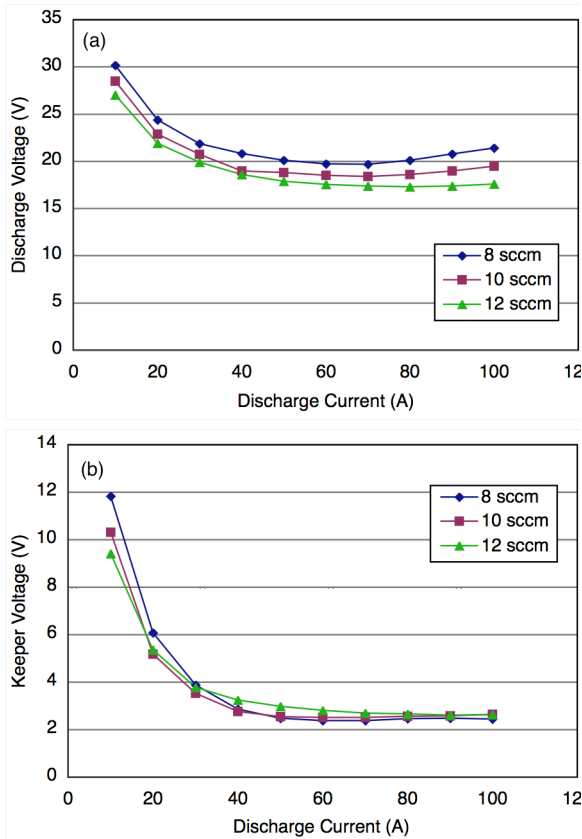


Figure 9. Discharge voltage (a) and keeper voltage (b) for the 1.5-cm cathode at three xenon flow rates.

temperature. In this case, the voltage drop in the cathode plasma increases to provide sufficient heating, which increases the measured discharge voltage.

Utilizing a longer graphite tube to reduce heat loss to the mounting structure, and increasing the heat shielding to reduce the radiation heat loss, makes it easier for the self-heating mechanism to maintain the insert temperature at low currents. The smaller cathode shown in Fig. 5 can run at 5 A or below, and also is capable of 60 A of emission current at a temperature of 1700 °C. These high emission current densities and discharge currents are routinely achieved with LaB₆ cathodes^{16,23}. The 1.5-cm-dia. cathode has 5 cm² of exposed insert area, and so is capable of producing the measured 100 A of discharge current at an emission current density of 20 A/cm² and a temperature of 1700 °C. The 2.0-cm dia. cathode, in comparison, has either 10 or 20 cm² of insert area depending on the insert length selected, and is capable of well over 200 A of emission.

To understand the electron emission processes of the LaB₆ insert in this size hollow cathode, plasma density, potential and electron temperature profiles were taken by the interior fast-scanning probe. Previous problems with melting of the probe in the high-density plasma inside the cathode insert at discharge currents over 30 A were mitigated by increasing scan speed and scanning length such that probe was could be kept inside a protective tube mounted the cooler base-flange between fast-scans. This lowered the probe temperature before insertion and protected the probe tip from erosion and material deposition from the cathode plasma. Figure 10 shows the plasma density profiles calculate from the internal scanning probe data at discharge currents from 20 to 100 A and three

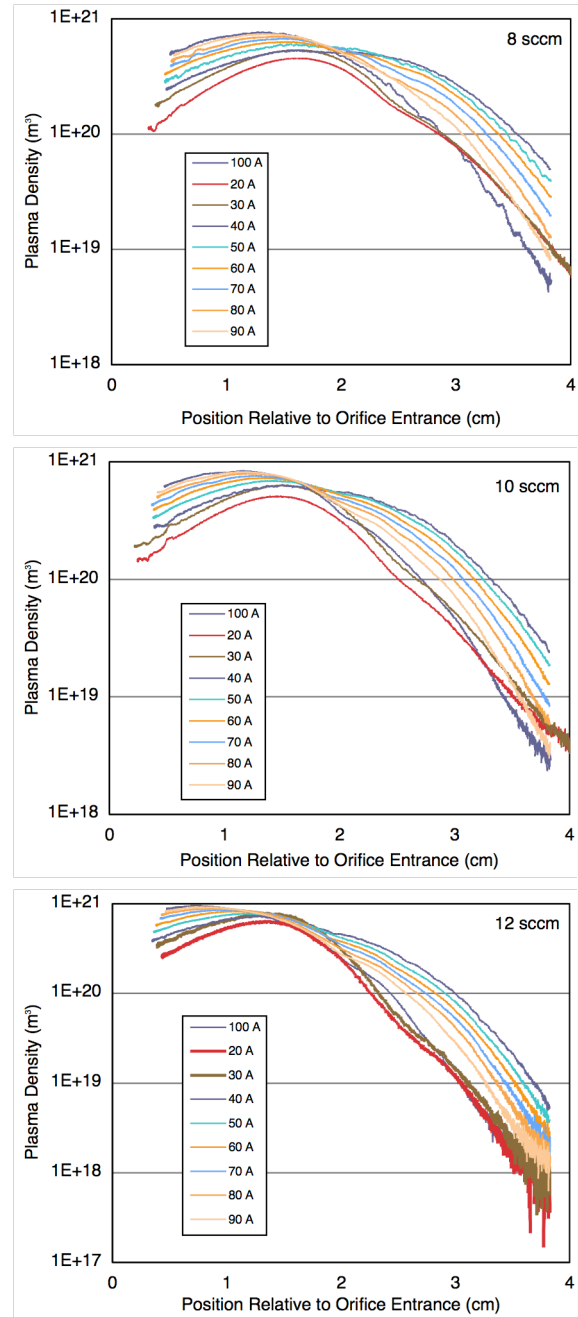


Figure 10. Density profiles inside the insert at discharge currents up to 100 A for the 1.5-cm cathode at three xenon flow rates.

xenon flow rates. The plasma profile in the LaB₆ cathode is very broad, and the plasma is in good contact with the entire insert length. In addition, the plasma density inside the insert is very high, and is sufficient all along the 2.5-cm insert length to avoid space-charge limitations on the emitted electron current density well in excess of 20 A/cm². Therefore, the insert is operating in the thermally-limited emission regime and the emission will be fairly uniform along the insert length if the temperature is constant. Increases in discharge current and gas flow rate tend to push the plasma density peak toward the orifice, further flattening the profile. Since the plasma is in contact with the entire insert and LaB₆ has a good thermal conductivity²⁶, the temperature variation along the insert is expected to be small and the emission fairly uniform.

The probe electronics system was also configured to record Langmuir traces so that potential and electron temperature profiles could be obtained. Figure 11 shows the plasma potential (top) and electron temperature (bottom) profiles inside the 1.5-cm cathode at a discharge current of 100 A. The potential profile behavior is similar to that observed at lower currents with peak voltages in excess of 10 V. The plasma potential profile at 100 A of discharge current is only about 1 V higher than that measured at 50 A of discharge current. The electron temperatures are also 50% higher than the values measured at 50 A of discharge current, even though the profile slopes and shapes are similar. The electron temperatures are significantly higher than observed in NSTAR and NEXIS cathodes^{36,37}, which is due to the lower neutral pressure in the LaB₆ insert region.

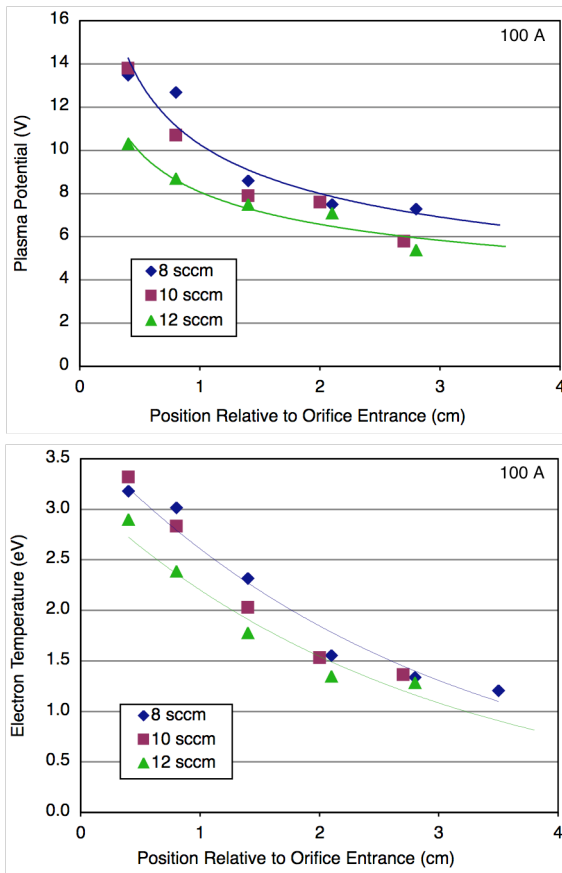


Figure 11. Plasma potential and electron temperature profiles in the 1.5-cm cathode at three xenon flow rates and 100 A.

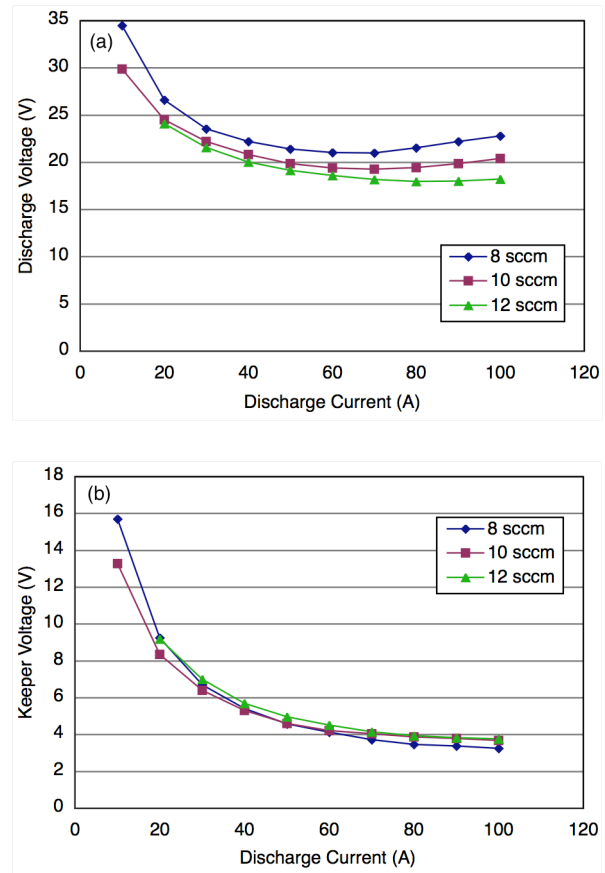


Figure 12. Discharge voltage (a) and keeper voltage (b) for the 2.0-cm cathode at three xenon flow rates.

B. 2.0-cm Cathode Performance

Figure 12 shows the discharge voltage (a) and keeper voltage (b) versus discharge current for the 2.0-cm cathode measured for currents of 10 to 100 A and three xenon gas flow rates. Like the smaller cathodes, at discharge currents below 20 A the discharge voltage was observed to increase and the cathode tended to cool off and stop operating after a short time. As seen in the figure, the discharge voltage increases at low current so that the voltage drop in the cathode plasma can increase to provide sufficient self-heating. The discharge voltage at low current is higher for the

2-cm cathode than for the 1.5-cm cathode, which is due to the higher heat loss associated with the larger radiating areas and conduction path for the larger cathode. At high current where radiation heat loss dominates, the two cathodes have nearly the same discharge voltage at the same flow because the orifice dimensions are the same.

Figure 13 shows the discharge voltage, keeper voltage and orifice plate temperature for the 2.0-cm cathode versus discharge current up to 250 A at a constant flow of 16 sccm. At low discharge currents, the discharge voltage decreases with current rapidly due to the self-heating issues, but also increases with discharge current at the high current levels. At 250 A of discharge current, a cathode flow rate of 20 sccm is required to keep the discharge voltage below 25 V in the test facility configuration. The orifice plate temperature shown in Fig. 13 is observed to increase proportionally to the discharge current. At 200 A of discharge current, the orifice plate is about 2350 °C, and at 250 A it is 2480 °C. The high orifice plate temperature observed in this cathode geometry is because the orifice plate is not in good contact with the graphite tube and so must radiate all the incident power from the local discharge. As will be discussed below, the orifice plate temperature in this range is not a major issue for tungsten material in terms of evaporation or life.

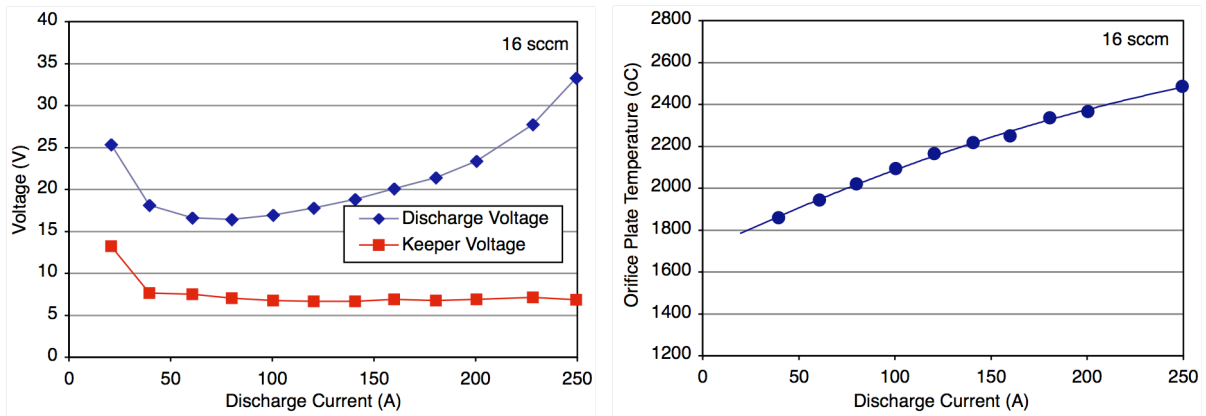


Figure 13. Discharge voltage and keeper voltage (left), and orifice plate temperature (right) for the 2.0-cm cathode.

V. Discussion

A. Cathode Life

The 1.5-cm dia. cathode is nominally rated for discharge currents up to 100 A where the temperature of the LaB_6 insert is expected to be about 1700 °C and the orifice plate temperature is measured to be below 2000 °C. As seen in Fig. 11, the plasma potential inside the insert region is less than 15 V over the range of currents tested, which means that sputtering of the LaB_6 insert is not an issue and the lifetime is due primarily to evaporation. It is observed that the emitting surface stoichiometry of the LaB_6 is modified by the plasma discharge, appearing more gray in color indicative of LaB_4 formation, which is likely due to redeposition of the easily ionized lanthanum as it evaporates from the surface. The work function of LaB_4 is actually lower¹⁸ than that of LaB_6 , so the cathode is expected to run cooler and longer in this condition. Nevertheless, a conservative life estimate can be made based on evaporation³⁸ and is shown in Fig. 14 as a function of discharge current for the two cathodes. For the 1.5-cm cathode running at 100 A, the evaporation-limited life is calculated to be about 12,000 hours. The 2.0-cm cathode is calculated to achieve 20,000 hours of life at currents of 200 A. Since the plasma density inside these cathodes extends well past the insert length, there will be no space charge limitation on the emission current

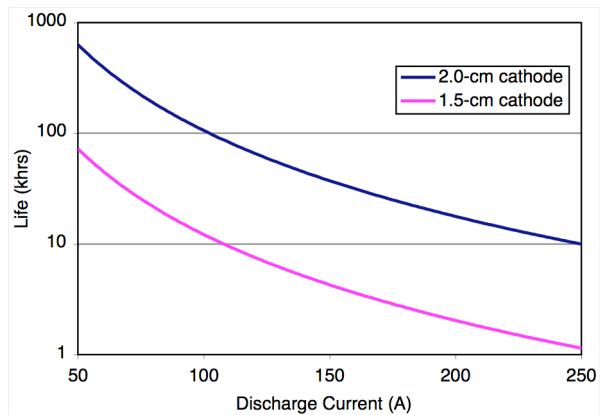


Figure 14. Evaporation-limited life of the two LaB_6 hollow cathodes as a function of discharge current.

if longer inserts are used. Longer life can then be obtained for both cathodes by utilizing a longer insert in the same cathode geometry. If the life is still insufficient for a given application, then the cathode diameter will have to be increased in order to provide larger electron emission areas and drop the insert temperature and evaporation rate. Any redeposition of the evaporated LaB₆ material will have a similar positive effect in extending the life. An evaluation of the redeposition and life of these cathodes is underway.

B. Internal Parameters

The high current cathodes utilize relatively large diameter orifices that reduce the pressure inside the cathode compared to the well-known smaller hollow cathodes such as the NSTAR cathode³⁷. The internal pressure in the 1.5-cm LaB₆ cathode was measured upstream of the insert region by a capacitive manometer connected to the cathode tube 15 cm from the orifice plate entrance. Neutral pressure profiles inside the insert region are then calculated using a 1-D Poiseuille-flow model described in Appendix B of Ref. [39]. The model uses variable diameter disks and calculates the pressure in each disk moving upstream from the cathode orifice using

$$P_1 = \left(P_2^2 + \frac{0.78Q\zeta T_r l}{d^4} \right)^{1/2}, \quad (4)$$

where P_2 is the pressure of the downstream disk, Q is the xenon gas flow rate in sccm, l is the disk length, d is the disk diameter, $T_r = T(^{\circ}\text{K})/289.7$, and ζ is the viscosity of the xenon gas given by

$$\zeta = 2.3 \times 10^{-4} T_r^{(0.71+0.29/T_r)} \quad \text{for } T_r > 1. \quad (5)$$

The gas velocity is assumed to transition to sonic in the cathode orifice, and the gas temperature is increased over the thermal temperature of the insert by charge exchange with the plasma ions. The gas temperature in the insert region is then adjusted such that the calculated pressure upstream of the cathode matches the measurement by the capacitive manometer. The neutral pressure profiles calculated for the 1.5-cm dia. cathode are shown in Fig. 15. The non-uniform neutral profile occurs because of different internal diameters in the cathode structure. At the 10 sccm of flow, the neutral pressure in the middle of the insert region (corresponding to near the plasma density maximum) is about 1.5 Torr and falls to less than 1 Torr at the orifice. This is significantly lower than the pressures inside the NSTAR cathode³⁷ and results in the penetration of the plasma deep into the insert as seen in Fig. 10.

The very broad axial density profiles observed in the LaB₆ cathode insert region encourages comparisons with the predictions of some simple models of the cathode parameters³⁹ previously developed. The electron temperature inside the cathode for a relatively long plasma in 1-D is determined by the matching of the radial ion loss rate in the plasma due to diffusion with the ion generation rate. The solution to the radial diffusion equation for ions in collisionally dominated plasmas in cylindrical geometry results in an eigenvalue equation with a unique dependence on the electron temperature:

$$\left(\frac{r}{\lambda_{01}} \right)^2 n_o \sigma_i(T_e) \sqrt{\frac{8kT_e}{\pi m}} - D = 0, \quad (4)$$

where r is the internal radius of the insert, λ_{01} is the first zero of the zero-order Bessel function, n_o is the neutral density, σ_i is the ionization cross section averaged over a Maxwellian electron temperature and D is the diffusion coefficient. The diffusion in the radial direction in the insert region is ambipolar, and the ion mobility is limited by

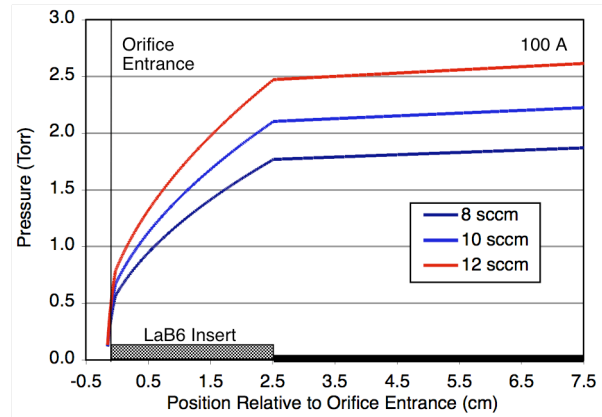


Figure 15. Pressure profiles inside the 1.5-cm LaB₆ hollow cathode at 100 A and three xenon gas flow rates.

resonant charge exchange (CEX) with the xenon neutral atoms. Since the electron mobility is much higher than the ion mobility, the ambipolar diffusion coefficient D_a is given by

$$D_a = \frac{e}{M} \frac{(T_i + T_e)}{\sigma_{CEX} n_o v_{scat}}, \quad (5)$$

where the ion and electron temperatures are given in electron volts and the effective velocity for scattering of the ions in the insert region is approximated by the ion thermal speed:

$$v_{scat} = \sqrt{\frac{kT_i}{M}}. \quad (6)$$

Equation 4 is then solved using Eqs. 5 and 6 for the average value of the electron temperature in the peak plasma-density region of the insert.

The density of the insert plasma can be estimated by a simple 0-D particle and energy balance model³⁹ that assumes fairly uniform plasma in the insert region. In the insert plasma, heating of the plasma is balanced by the energy loss

$$I_t \phi_s + RI_e^2 = I_i U^+ + \frac{5}{2} T_e I_e + (2T_e + \phi_s) I_r e^{-\phi_s/T_e}, \quad (7)$$

where I_t is the thermionic electron current given by Eq. 3, ϕ_s is the cathode sheath voltage, R is the plasma resistance, I_e is the hollow cathode discharge current, I_i is the total ion current generated in the insert region, U^+ is the ionization potential, T_e is the electron temperature (in volts), and I_r is the random electron flux at the sheath edge. In this case, excitation and radiation losses are ignored because the high-density plasma inside the hollow cathode is optically “thick” and the radiated energy is reabsorbed by the plasma. At the insert surface, power balance gives:

$$H(T) + I_t \phi_{wf} = I_i \left(U^+ + \phi_s + \frac{T_e}{2} - \phi_{wf} \right) + (2T_e + \phi_{wf}) I_r e^{-\phi_s/T_e}, \quad (8)$$

where $H(T)$ is the total heat lost by the insert due to radiation and conduction, and ϕ_{wf} is the cathode work function. The average plasma density can be found using Eqs. 7 and 8:

$$\bar{n}_e = \frac{RI_e^2 - \left(\frac{5}{2} T_e - \phi_s \right) I_e}{\left[f_n T_e \left(\frac{eT_e}{2\pi m} \right)^{1/2} eA e^{-\phi_s/T_e} + n_o e \langle \sigma_i v_e \rangle V (U^+ + \phi_s) \right]}, \quad (9)$$

where f_n is the edge to average plasma density ratio assumed to be near one for this relatively low pressure plasma. Finally, the sheath potential at the cathode surface³⁹ is found from solving Eq. 8 and particle balance equations:

$$\phi_s = \frac{H(T)}{I_e} + \frac{5}{2} T_e V + \phi_{wf} - I_e R. \quad (10)$$

Figure 16 shows the plasma density, potential and electron temperature data for the 1.5-cm LaB₆ hollow cathode operating at the condition 100 A and 10 sccm of cathode flow shown in Figs. 10 and 11. The average plasma density, potential and electron temperature predicted by Eqs. 4, 9 and 10, evaluated at the peak in the plasma density profile and using the neutral density at this location from Fig. 15, are also shown in Fig. 16. The predictions of the simple models agree reasonably well with the average parameters inside the insert region, and provide information

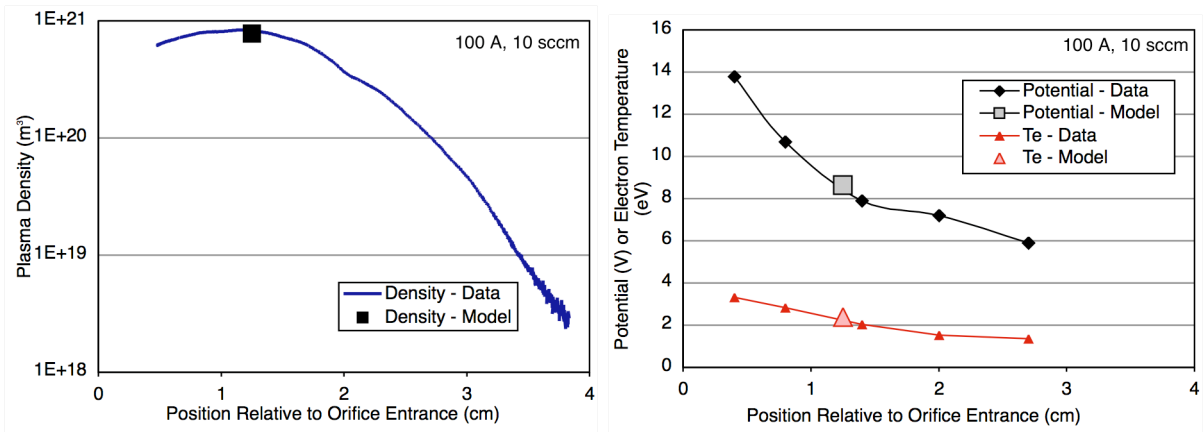


Figure 16. Comparison of predictions of the average value of the density, potential and electron temperature from simple models with the data from Figs. 10 and 11 for the cathode operating at 100 A of discharge current and 10 sccm xenon gas flow.

that is used in selection of the orifice and insert dimensions. Detailed modeling of the plasma profiles requires a 2-D code such as OrCA-2D⁴⁰, which has successfully modeled the plasma parameters for smaller cathodes in the past⁴¹. Simulations of the high current cathodes using this code are underway at this time.

C. Orifice Plate Heating

The cathode orifice plate was observed to operate at temperatures over 2000 °C at the high discharge currents reported here. This is significantly higher than lower current BaO-W cathodes and is attributed to both the high heat fluxes associated with high current operation and the lack of conduction cooling of the orifice in the present graphite-tube geometries. An early version of the 1.5-cm cathode was tested at discharge currents of 200 A for over 120 hours with a tantalum orifice plate. Figure 17 shows a photograph of the tantalum orifice plate at the end of this test. The cathode orifice diameter had enlarged by 11% and the tantalum surface had clearly recrystallized associated with high temperatures. Based on tantalum evaporation rates in the literature⁴², this change in the orifice diameter is expected for temperatures of nearly 2600 °C. Evaporation of the orifice plate would then limit the life of the 1.5-cm cathode to about a tenth that expected from insert evaporation. The orifice plate material was changed to tungsten, which has a significantly lower evaporation rate than tantalum at a given temperature, and the keeper orifice enlarged slightly to provide more radiation area from the cathode orifice plate. At 100 A, the 1.5-cm cathode orifice plate was found using the optical pyrometer to be at a temperature of only about 2000 °C, which is about 300° hotter than this insert at this current. This temperature would produce an evaporation change in the orifice diameter of 10% after 200,000 hours, which is not a significant life-limiting problem.

The 2.0-cm dia. cathode was designed with a tungsten orifice plate installed in a similar configuration as the 1.5-cm cathode with the graphite support tube. As shown in Fig. 13, the 2.0-cm cathode has an orifice plate temperature of about 2350 °C at 200 A of discharge current. Based on the tungsten evaporation rates published in the literature by Langmuir⁴³, this orifice plate temperature would produce in a 12% increase in the cathode orifice diameter after 20,000 hours. The orifice and insert then have similar lifetimes at this discharge current level, and the cathode is therefore expected to last for at least 20 khrs at 200 A of discharge current. If longer life or higher discharge currents are desired, the cathode tube can be made of a refractory metal and welded to the tungsten orifice plate as is done in standard hollow cathodes to provide conduction cooling of the orifice plate and operation a lower temperature.

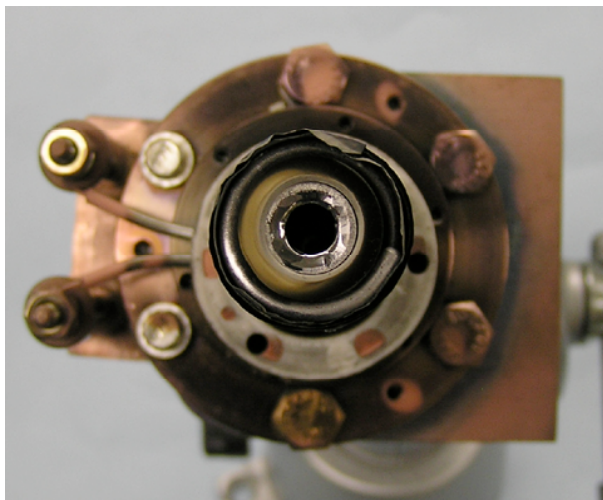


Figure 17. Photograph of the tantalum orifice plate after 120 hrs in the 1.5-cm cathode at 200 A of current.

D. Energetic Ion Production

During testing of both the 1.5-cm and 2.0-cm cathodes at currents in the 100 to 200 A range and cathode flows of ≤ 16 sccm, it was observed that a significant amount of copper was sputtered from the anode close to the cathode exit and the anode surface damaged. The conical anode shown in Fig. 8 was turned around 180° to provide more surface area to handle this ion bombardment and allow access for diagnostics. Figure 18 shows a photograph of the anode end that faces the cathode (tilted toward the camera) after operation to show the sputtered zone. Close to the cathode, the anode had molybdenum deposition in a region about 1 cm long, coming from the molybdenum plate seen on the right around the cathode keeper that protects the solenoid coil. Beyond that shiny Mo-ring, there is net erosion of the copper wall of the anode shown by a characteristic rough sputtered surface. It is clear that energetic ions are produced downstream of the keeper exit at these high discharge currents, which then bombard the anode and keeper surface. The keeper is made of graphite and no significant erosion has been detected to date.

Energetic ion production in the plume of various hollow cathodes has been previously at JPL^{44,45}. While several mechanisms for producing high energy ions have been proposed, the ion quantity and energy have been correlated to ionization instabilities in the near-cathode plume⁴⁶. Some fraction of these ions flow back toward the cathode and cause keeper erosion, and the remainder flow radially and axially away from the cathode and can cause damage to other thruster components such as the anodes and grids. To mitigate the copper erosion, a tungsten liner was installed to cover the first 10 cm of the anode. Future work will re-examine the source of these energetic ions under the high current discharge conditions, and experiments will be made to mitigate their production and affect on thruster and test stand components.

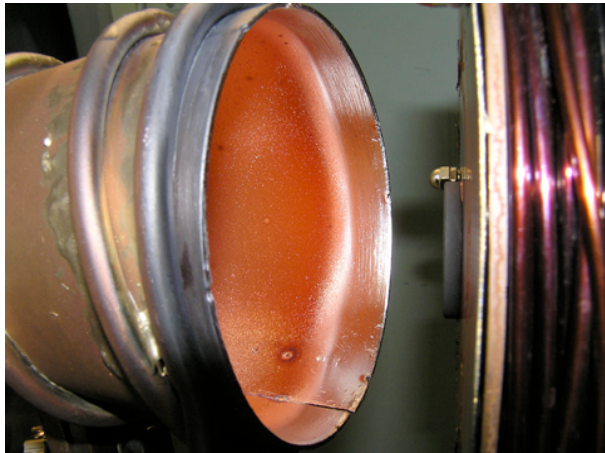


Figure 18. Photograph of the discharge anode after testing the 2.0-cm cathode at 200 A of current.

VI. Conclusion

The successful development of a reliable, robust LaB₆ hollow cathode that operates in the range of 5 to 60 A and has run several Hall thrusters at various institutions in the US has spurred the development of higher current versions for very high power thrusters. Two cathodes, a 1.5-cm dia. version and a 2.0-cm dia. version, have been built and tested at discharge currents ranging from 10 to 250 A. The tantalum sheathed heater technology based on Al₂O₃-powder insulation has proven to be reliable in successfully heating all of these large, higher temperature cathodes to ignition conditions. The cathodes have lifetimes in the 10 to 20 khrs range depending on their operating conditions, and experiments have shown the path to even higher currents and longer lifetimes if required by future missions.

Acknowledgments

The research described in this paper was carried out by the Jet Propulsion Laboratory, California Institute of Technology, under a contract with the National Aeronautics and Space Administration. Copyright 2011. All rights reserved.

References

¹J.R. Brophy, R. Gershman, N. Strange, D. Landau, R. Merrill, T. Kerslake, "300-kW Solar Electric Propulsion System Configuration for Human Exploration of Near-Earth Asteroids", AIAA-2011-551, 47th AIAA Joint Propulsion Conference, San Diego, California, July 31-3, 2011.

²N. Strange, R. Merrill, D. Landau, B. Drake, J.R. Brophy, R. Hofer, "Human Missions to Phobos and Deimos Using Combined Chemical and Solar Electric Propulsion", AIAA-2011-5663, 47th AIAA Joint Propulsion Conference, San Diego, California, July 31-3, 2011.

³C. Garner, M. Rayman, J. Brophy, "In-Flight Operation of the Dawn Ion Propulsion System: Status at One Year From the Vesta Rendezvous", AIAA-2010-7111, 47th AIAA Joint Propulsion Conference, San Diego, California, July 31-3, 2011.

- ⁴K. Nishiyama, S. Hosoda, H. Koizumi, Y. Shimizu, I. Funaki, H. Kuninaka, M. Bodendorfer, J. Kawaguchi, D. Nakata, "Hayabusa's Way Back to Earth by Microwave Discharge Ion Engines", AIAA-2010-6862, 47th AIAA Joint Propulsion Conference, San Diego, California, July 31-3, 2011.
- ⁵C. Koppel, M. Cramayel, F. Marchandise, M. Prioul, D. Estuglier, F. Darnon, "The Smart-1 Electric Propulsion Subsystem Around the Moon: In Flight Experience", AIAA-2005-3671, 41st AIAA Joint Propulsion Conference and Exhibit, Tucson, Arizona, July 10-13, 2005.
- ⁶J.R. Brophy, "Asteroid Return Mission Feasibility Study", AIAA-2011-5665, 47th AIAA Joint Propulsion Conference, San Diego, California, July 31-3, 2011.
- ⁷R.Levi, "Improved impregnated cathode", J. Appl. Phys., **26**, 1955, p.639.
- ⁸J.L.Cronin, "Modern dispenser cathodes", IEE Proc., **128**, 1981, pp. 19-32.
- ⁹M.J. Patterson, "Space Station Cathode Design, Performance, and Operating Specifications," NASA/TM-1998-206529, May 1998.
- ¹⁰B.A. Arkhopov and K.N. Kozubsky, "The development of the cathode compensators for stationary plasma thrusters in the USSR", 22nd International Electric Propulsion Conference, paper IEPC-91-023, Viareggio, Italy Oct. 14-17, 1991.
- ¹¹V. Kim, "Electric propulsion activity in Russia," IEPC-2001-005, 27th International Electric Propulsion Conference, Pasadena, CA, October 14-19, 2001.
- ¹²D. Pidgeon, R. Corey, B. Sauer, M. Day, "Two Years of On-Orbit Performance of SPT-100 Electric Propulsion", AIAA-2006-5353, 24th AIAA International Communications Satellite Systems Conference, San Diego, California, June 11-14, 2006.
- ¹³R. Corey, N. Bascon, J. Delgado, G. Gaeta, S. Munir, J. Lin, "Performance and Evolution of Stationary Plasma Thruster Electric Propulsion for Large Communications Satellites", AIAA-2010-8688, 28th AIAA International Communications Satellite Systems Conference (ICSSC-2010), Anaheim, California, Aug. 30-2, 2010.
- ¹⁴D.M. Goebel and R. Watkins, "LaB₆ Hollow Cathodes for Ion and Hall Thrusters", AIAA-2005-4239, 41st Joint Propulsion Conference, Tucson, AZ, July 11-13, 2005.
- ¹⁵D.M. Goebel, R.M. Watkins and K. Jameson, "LaB₆ Hollow Cathodes for Ion and Hall Thrusters", AIAA Journal of Propulsion and Power, **23**, No.3, p.527-528 (2007).
- ¹⁶D.M. Goebel and R.M. Watkins, "Compact Lanthanum Hexaboride Hollow Cathode", Rev. Sci. Instrum., **81**, 083504, (2010).
- ¹⁷J.M. Lafferty, "Boride cathodes", J. Appl. Phys., **22**, 1951, pp. 299-309.
- ¹⁸Storms and Mueller, "A study of surface stoichiometry and thermionic emission using LaB₆, J. Appl. Phys., **50**, 1979, pp. 3691-3698.
- ¹⁹E. Storms and B. Mueller, "Phase relationship, vaporization and thermodynamic properties of the lanthanum-boron system", J. Chem. Phys. **82**, 1978, pp.51-59.
- ²⁰D. Jacobson and E.K. Storms, "Work function measurement of lanthanum-boron compounds", IEEE Trans. Plasma Sci., **6**, 1978, pp. 191-199.
- ²¹J. Pelletier and C. Pomot, "Work function of sintered lanthanum hexaboride", Appl. Phys. Lett., **34**, 1979, pp.249-251.
- ²²D.M. Goebel, J.T. Crow and A.T. Forrester, "Lanthanum hexaboride hollow cathode for dense plasma production", Rev. Sci. Instrum., **49**, 1978, pp.469-472.
- ²³D.M. Goebel, Y. Hirooka and T. Sketchley, "Large area lanthanum hexaboride electron emitter", Rev. Sci. Instrum., **56**, 1985, pp.1717-1722.
- ²⁴O.W. Richardson, "Electron theory of matter", Philips Mag., **23**, 1912, pp.594-627.
- ²⁵A.T. Forrester, *Large Ion Beams*, Wiley-Interscience, NY, 1988.
- ²⁶W. H. Kohl, *Handbook of Materials and Techniques for Vacuum Devices*, Reinhold, NY (1967).
- ²⁷K.N. Leung, P.A. Pincosy, and K.W. Ehlers, "Directly heated lanthanum hexaboride filaments", Rev. Sci. Instrum., **55**, 1984, pp.1064-1068.
- ²⁸L.J. Favreau, "Cataphoretic Coating Lanthanum Boride on Rhenium Filaments", Rev. Sci. Instrum., **36**, 1965, pp.856-857.
- ²⁹A.N. Boers, "Electron Gun Using Long-Life Lanthanum Hexaboride Cathode", J. Appl. Phys., **38**, 1967, pp.1991-1992.
- ³⁰J.L. Cronin, "Practical aspects of modern dispenser cathodes", Microwave Journal, Sept. 1979.
- ³¹H.E. Gallagher, "Poisoning of LaB₆ cathodes", J. Appl. Phys., **40**, 1969, pp. 44-51.
- ³²G.C. Soulas, "Status of Hollow Cathode Heater Development for the Space Station Plasma Contactor", 30th Joint Propulsion Conference, Indianapolis, IN, June 27-29, 1994.
- ³³W.G. Tighe, K. Freick and K.R. Chien, "Performance Evaluation and Life Test of the XIPS Hollow Cathode Heater", AIAA 2005-4066, 41st Joint Propulsion Conference, Tucson, AZ, July 10-13, 2005.
- ³⁴Catalog item from Idaho Labs, Idaho Falls, Idaho.
- ³⁵C.H. Chen, et al., "Structural refinement and thermal expansion of hexaborides", Journal of Alloys and Compounds, **366**, L6-L8 (2004).
- ³⁶D.M. Goebel, K. Jameson, R. Watkins, I. Katz, "Hollow Cathode and Keeper-Region Plasma Measurements Using Ultra-Fast Miniature Scanning Probes", AIAA-2004-3430, 40th AIAA Joint Propulsion Conference, Fort Lauderdale, FL, July 11-14, 2004.
- ³⁷K. Jameson, D.M. Goebel, R. Watkins, "Hollow Cathode and Keeper-Region Plasma Measurements", AIAA-2005-3667, 41st AIAA Joint Propulsion Conference, Tucson, AZ, July 10-13, 2005.
- ³⁸D.M. Goebel, et al., "Extending hollow cathode life for electric propulsion in long-term missions", AIAA Paper 2004-5911, Space 2004 Conference, San Diego, CA Sept. 28-30, 2004.

- ³⁹D.M. Goebel and I. Katz, *Fundamentals of Electric Propulsion; Ion and Hall Thrusters*, John Wiley and Sons, NJ 2008.
- ⁴⁰I. Mikellides, I.Katz, D.M.Goebel, K.K. Jameson “Plasma Processes Inside Orificed Hollow Cathodes”, *Physics of Plasmas*, **13**, 063504 (2006).
- ⁴¹I. Mikellides, I. Katz, D.M. Goebel, “Numerical Simulation of the Hollow Cathode Discharge Plasma Dynamics”, IEPC-2005-200, 29th International Electric Propulsion Conference, Princeton University, Oct. 31-Nov. 4, 2005.
- ⁴²D.B. Langmuir and I. Malter, *Phys.Rev.* **55**, 748-749 (1939).
- ⁴³I. Langmuir, *Phys.Rev.* **7**, 235-271 (1916).
- ⁴⁴D.M. Goebel, K. Jameson, I. Katz, I. Mikellides, J. Polk, “Energetic Ion Production and Keeper Erosion in Hollow Cathode Discharges” IEPC-2005-266, 29th International Electric Propulsion Conference, Princeton University, Oct. 31-Nov. 4, 2005.
- ⁴⁵D.M. Goebel, D.M. Goebel, K. Jameson, I. Katz and I. Mikellides, “Potential Fluctuations and Energetic Ion Production in Hollow Cathode Discharges”, *Physics of Plasmas*, **14**, 103508 (2007).
- ⁴⁶D.M. Goebel, K. Jameson, I. Katz and I. Mikellides, “Plasma Potential Behavior and Plume Mode Transitions in Hollow Cathode Discharges” IEPC-2007-27, 30th International Electric Propulsion Conference, Florence, Italy, Sept. 17-20, 2007.